PENNY-SHAPED CRACK IN A FIBER-REINFORCED MATRIX

by

T.V. NARAYANAN and F. ERDOGAN

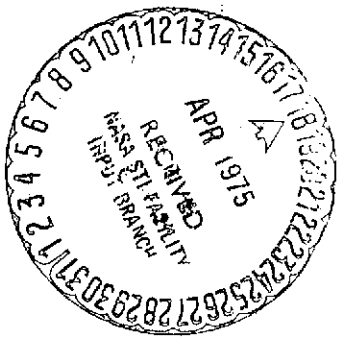

October 1974

NATIONAL AERONAUTICS AND SPACE ADMINISTRATION

GRANT NGR 39-007-011

Penny-Shaped Crack in a Fiber-Reinforced Matrix*

by

T.V. Narayanan and F. Erdogan

Lehigh University, Bethlehem, Pa.

Abstract

Using the slender inclusion model developed earlier the elastostatic interaction problem between a penny-shaped crack and elastic fibers in an elastic matrix is formulated. For a single set and for multiple sets of fibers oriented perpendicularly to the plane of the crack and distributed symmetrically on concentric circles the problem is reduced to a system of singular integral equations. Techniques for the regularization and for the numerical solution of the system are outlined. For various fiber geometries numerical examples are given and distribution of the stress intensity factor along the crack border is obtained. Sample results showing the distribution of the fiber stress and a measure of the fiber-matrix interface shear are also included.

1. INTRODUCTION

The general problem of an elastic matrix containing a penny-shaped crack and reinforced by filaments of finite length was introduced in [1] and [2]. In this problem the external loads were applied to the matrix at "infinity" and there were severe stress concentrations around the end points of the filaments, meaning that the load transfer from the matrix to the filaments took place mainly around the ends of the filaments. On the other hand, if the medium containing the crack is a fiber-reinforced composite with fibers extending into the loading grips, outside the stress perturbation zone

*This work was supported by NSF under the Grant GK-42771X and NASA Langley Research Center under the Grant NGR-39-007-011.

of the crack the fiber-matrix interface shear will be zero. In this case the region of load transfer between the fiber and the matrix will be restricted to the neighborhood of the crack (approximately four crack diameters along the fiber), and the nature of the governing integral equations will be somewhat different than that of the filament problem.

In this paper the problem of a fiber-reinforced elastic matrix containing a penny-shaped crack will be formulated and solved under certain simplifying assumptions regarding the geometry of the medium. The main assumptions are (a) the crack is a plane circular (penny-shaped) internal crack; (b) the fibers are circular elastic cylinders which are perfectly bonded to the matrix, are oriented perpendicular to the plane of the crack, and are symmetrically distributed on circles concentric with the crack; (c) the composite system is loaded perpendicular to and away from the crack; (d) the fiber diameter is relatively small compared to other lateral dimensions so that the assumption of local axisymmetry in fiber stresses in considering the fiber-matrix displacement compatibility and the use of the filament model developed in [1] are justified; and (e) the Poisson's ratios of the matrix and the fiber are equal so that the reinforcing fiber may be replaced by an auxiliary inclusion having the elastic constants $E_f - E$ and ν and by a layer of body forces [1], where E,ν are the elastic constants of the matrix and E_f is the Young's modulus of the fibers. The technique developed in the paper is quite straightforward and may easily be applied to

any number of fiber systems each distributed symmetrically around the crack. As the results indicate, when the number of fibers is increased the stress state around the leading edge of the crack approaches an axisymmetric one. Thus reformulating the problem as an axisymmetric one, substantial simplification in the solution can be achieved.

2. FORMULATION OF THE PROBLEM

First we consider a simple set of fibers distributed symmetrically around the crack as shown in Figure 1. As in [2] the unknown function in the problem is the layer of body forces $Z(z)$ imbedded on the fiber-matrix interface which can be obtained from the displacement or strain continuity condition along the interface. If $Z(z)$ is the layer of body forces acting on the matrix then the cylindrical auxiliary fiber of infinite length is subjected to axial surface tractions of magnitude $-Z(z)$. Assuming a fixed-grip type of loading at infinity the equilibrium condition of the auxiliary fiber gives

$$\pi r_o^2 \sigma_o \frac{E_f - E}{E} - 2\pi r_o \int_z^\infty Z(t)dt - \pi r_o^2 \sigma^f(z) = 0 \qquad (1)$$

where r_o is the fiber radius, σ_o the stress acting on the matrix at $z = \mp\infty$, σ^f the stress acting on the auxiliary fiber, and E_f and E the moduli of the fiber and the matrix, respectively. From (1) the strain of the auxiliary fiber may be expressed as

$$\varepsilon_z^f(z) = \frac{\sigma^f(z)}{E_f - E} = \frac{\sigma_o}{E} - \frac{2}{r_o(E_f - E)} \int_z^\infty Z(t)dt. \qquad (2)$$

The strain in the matrix ε_z^m may be obtained from the superposition of the solutions of four problems shown in Figure 2. Thus, the integral equation for Z may be obtained by writing

$$\varepsilon_z^m = \varepsilon_z^a + \varepsilon_z^b + \varepsilon_z^c + \varepsilon_z^d = \varepsilon_z^f, \quad (-\infty<z<\infty). \tag{3}$$

Similar to the derivation given in [2], the strains $\varepsilon_z^a,..,\varepsilon_z^d$ may be expressed as (Figures 1 and 2)

$$\varepsilon_z^a = \sigma_o/E, \tag{4}$$

$$\varepsilon_z^c(z) = \frac{1}{EC_1}\int_{-\infty}^{\infty}\left[\frac{1}{t-z} + k_c(z,t)\right]Z(t)dt, \quad (-\infty<z<\infty), \tag{5}$$

$$k_c(z,t) = \frac{2r_o}{\rho_o}\,\frac{E(k)-1}{t-z} + \frac{1}{\rho_o}\,\frac{2r_o-\rho_o}{t-z}$$
$$+ \frac{2r_o\gamma(t-z)}{\rho_o^3}\,[2E(k) - K(k)]$$
$$+ \pi r_o(t-z)\sum_{i=2}^{n}\frac{1}{[d_i^2 + (t-z)^2]^{3/2}}\,(1-2\gamma$$
$$+ \frac{3\gamma(t-z)^2}{d_i^2 + (t-z)^2}),$$

$$\gamma = 1/(3-4\nu), \quad C_1 = 4\pi(1-\nu)/[(1+\nu)(3-4\nu)],$$

$$k = 2r_o/\rho_o, \quad \rho_o^2 = 4r_o^2 + (t-z)^2,$$

$$d_i = b[2(1-\cos\frac{2\pi(i-1)}{N})]^{\frac{1}{2}}, \quad (i = 2,..,N)$$

$$\varepsilon_z^b(r,z) = -\frac{1+\nu}{E}(2/\pi)^{\frac{1}{2}}\sigma_o[(1-2\nu)F_o(r,|z|) + |z|G_o(r,|z|)],$$
$$(|z|\geq 0), \tag{6}$$

$$\varepsilon_z^d(r,\theta,z) = -\frac{1+\nu}{E}(2/\pi)^{\frac{1}{2}} \sum_{n=0}^{\infty} a_n b_n \cos(nN\theta)*$$

$$*[(1-2\nu) F_n(r,|z|) + |z| G_n(r,|z|)], (|z| \geq 0) \quad (7)$$

$$F_n(r,z) = \int_0^{\infty} s^{\frac{1}{2}} J_{nN}(rs) J_{nN+3/2}(s) e^{-sz} ds, (z>0; n=1,2...) \quad (8)$$

$$G_n(r,z) = \int_0^{\infty} s^{3/2} J_{nN}(rs) J_{nN+3/2}(s) e^{-sz} ds, (z>0, n=0,1,2,..) \quad (9)$$

$$a_n = 2^{-2mN} \sum_{k=0}^{mN} \binom{2nN+1}{k} \frac{(-1)^{n-k}}{2n-2k+1}, \quad (10)$$

$$b_o = \frac{1}{\pi a^2} \int_0^a \int_0^{2\pi} p(r,\theta) r dr d\theta , \quad (11)$$

$$b_n = \frac{2(nN+1)}{\pi a} \int_0^a \int_0^{2\pi} p(r,\theta) \left(\frac{r}{a}\right)^{nN+1} \cos(nN\theta) dr d\theta, \quad (12)$$

$$p(r,\theta) = \frac{r_o}{4(1-\nu)} \int_{-\infty}^{\infty} Z(t) dt \sum_{m=1}^{N} \frac{1}{\rho_m^3}\left(1-2\nu + \frac{3t^2}{\rho_m^2}\right) dt, \quad (13)$$

$$\rho_m^2 = r^2 - 2br \cos\left(\theta - \frac{2\pi m}{N}\right) + b^2 + t^2 \quad (14)$$

where a is the radius of the crack which, in this paper, is assumed to be the length unit, K(k) and E(k) are the complete elliptic integrals, N is the number of the equally spaced fibers around the crack, b is the distance of the fibers from the crack center (Figure 1), and (r,θ,z) are the cylindrical coordinates shown in Figure 1, $\theta=0$ corresponding to fiber 1.

Substituting now from (2) and (4-7) into (3) with r=b and $\theta=0$ we find an integral equation of the following form to determine the unknown function Z(z):

$$\int_{-\infty}^{\infty} \frac{Z(t)}{t-z} dt + \int_{-\infty}^{\infty} k(z,t) Z(t) dt = f(z), \quad (-\infty<z<\infty), \quad (15)$$

where $f(z)$ is a known function and the known kernel $k(z,t)$ has an additional logarithmic singularity. after determining the body force distribution $Z(z)$, it was shown in [1] that the quantities of more physical interest, namely the interface shear σ_s and the total fiber stress σ_f may be obtained from

$$\sigma_s(z) = - \frac{E_f}{E_f - E} Z(z), \quad (-\infty<z<\infty), \tag{16}$$

$$\sigma_f(z) = \sigma^f(z) + \sigma_z{}^m(z), \quad (-\infty<z<\infty) \tag{17}$$

where σ^f is the stress in the auxiliary fiber and σ^m in the matrix. The matrix stress is obtained from the superposition shown in Figure 3. Thus,

$$\sigma_z{}^m(z) = \sigma_o + \sigma_z{}^b(b,z) + \sigma_z{}^c(b,z) + \sigma_z{}^d(b,z), \quad (-\infty<z<\infty) \tag{18}$$

where

$$\sigma_z{}^b(b,z) = - \sigma_o(2/\pi)^{\frac{1}{2}}[F_o(b,|z|) + |z|G_o(b,|z|)], \tag{19}$$

$$\sigma_z{}^c(b,z) = \frac{ro}{4(1-\nu)} \int_{-\infty}^{\infty} Z(t)\,(t-z)dt\{\frac{1-2\nu}{[r_o{}^2 + (t-z)^2]^{3/2}} + \frac{3(t-z)^2}{[r_o{}^2 + (t-z)^2]^{5/2}} + \sum_{i=2}^{N} [\frac{1-2\nu}{[d_i{}^2 + (t-z)^2]^{3/2}} + \frac{3(t-z)^2}{[d_i{}^2 + (t-z)^2]^{5/2}}]\}, \tag{20}$$

$$\sigma_z{}^d(b,z) = - (2/\pi)^{\frac{1}{2}} \sum_{o}^{\infty} a_n b_n [F_n(b,|z|) + |z|G_n(b,|z|)]. \tag{21}$$

Other quantities of physical interest are the crack opening displacement $u_z(r,\theta, +0)$ and the stress intensity factor along the leading edge of the crack. Referring to [2]

and Figure 2 u_z may be expressed as

$$u_z(r,\theta,+0) = u_z^{b}(r,+0) + u_z^{d}(r,\theta,+0)$$

$$= \frac{2(1-\nu^2)}{E}(2/\pi)^{\frac{1}{2}}\left[\sigma_o H_o(r,0) + \sum_{n=0}^{\infty} a_n b_n \cos(nN\theta)\, H_n(r,0)\right], \quad (0\leq r<1,\ 0\leq\theta<2\pi), \tag{22}$$

where

$$H_n(r,z) = \int_0^{\infty} s^{-\frac{1}{2}} J_{nN}(rs) J_{nN+3/2}(s) e^{-zs}\, ds, \quad (z>0). \tag{23}$$

From (see [3])

$$H_n(r,+0) = \begin{cases} \dfrac{r^{nN}(1-r^2)^{\frac{1}{2}}}{\sqrt{2}\,\Gamma(3/2)}, & (0\leq r<1), \\ 0, & (1<r<\infty) \end{cases} \tag{24}$$

we obtain

$$u_z(r,\theta,+0) = \frac{4(1-\nu^2)}{\pi E}(1-r^2)^{\frac{1}{2}}\left[\sigma_o + \sum_{n=0}^{\infty} a_n b_n r^{nN}\cos(nN\theta)\right], \quad (0\leq r<1, 0\leq\theta<2\pi). \tag{25}$$

Using now the definition of the stress intensity factor as

$$k_1(\theta) = \lim_{r\to 1}\sqrt{2(r-1)}\,\sigma_z^{m}(r,\theta,0)$$

$$= -\lim_{r\to 1}\frac{E}{2(1-\nu^2)}\sqrt{2(1-r)}\,\frac{\partial}{\partial r}u_z^{m}(r,\theta,+0), \tag{26}$$

we find

$$k_1(\theta) = (2/\pi)\left[\sigma_o + \sum_{n=0}^{\infty} a_n b_n \cos(nN\theta)\right], \quad (0\leq\theta<2\pi) \tag{27}$$

Note that because of symmetry the forward and anti-plane shear components of the stress intensity factor (k_2 and k_3) will be zero.

3. MULTIPLE SETS OF FIBERS

The analysis developed for a single set of fibers may easily be extended to multiple sets distributed with equal angular spacings on concentric rings around the penny-shaped crack. Consider the geometry given in Figure 3 and again let the fibers be oriented perpendicular to the plane of the crack. Let M be the number of concentric rings carrying the fibers, b_j,(j=1,..,M) the radius of the jth ring, N_j,(j=1,..,M) the number of the fibers on the jth ring*, and r_j and E_j,(j=1,..,M) the radius and the Young's modulus of the fibers in the jth set. The unknown functions will now be the layers of body forces $Z_j(z)$, (j=1,..,M) imbedded in the fiber-matrix interfaces and the strain continuity conditions expressed for a representative fiber in each set will give the necessary system of integral equations to determine these function. Thus, in this case (dropping the subscript z) the condition (3) is modified to read

$$\varepsilon_j^{f}(z) = \varepsilon_j^{m}(b_j,\theta_j,z) = \varepsilon^{a}(z) + \varepsilon^{b}(b_j,z) + \varepsilon_j^{c}(b_j,\theta_j,z) + \varepsilon_j^{d}(b_j,\theta_j,z), \quad (j=1,..,M;\ -\infty<z<\infty) \tag{28}$$

*Here it is assumed that the numbers N_j are either equal or multiples of each other and the fibers are distributed in such a way that the body forces (or the fiber stresses) in each set is the same. Otherwise, any deviation from symmetry will cause the fiber stresses in a given set to be different and the total number of unknown functions to be much greater than the number of sets M.

where θ_j is the angular orientation of the representative fiber in the jth set. The strain in the auxiliary fiber, ε_j^f may be obtained from (2) by replacing ε_z^f, E_f, and Z by ε_j^f, E_j, and Z_j, respectively. Referring to Figures 2 and 3, it is clear that in the superposition the axisymmetric strain components in the matrix ε^a and ε^b (which depend only on σ_o) will be the same as that found for the single set of fibers in the previous section and are given by (4) and (6).

Referring again to Figures 3 and 2c, if we let the axial strain in the matrix at a location of a representative fiber from the jth set (i.e., at $r=b_j$, $\theta=\theta_j$) due to all the body forces $Z_i(z)$ imbedded in the fiber-matrix interfaces on the ith ring be $\varepsilon_{ji}^c(b_j,\theta_j,z)$, the third term in (28) becomes

$$\varepsilon_j^c(b_j,\theta_j,z) = \sum_{i=1}^{M} \varepsilon_{ji}^c(b_j,\theta_j,z),$$

$$(j=1,..,M;\ -\infty<z<\infty). \tag{29}$$

Similarly,

$$\varepsilon_j^d(b_j,\theta_j,z) = \sum_{i=1}^{M} \varepsilon_{ji}^d(b_j,\theta_j,z),\ (j=1,..,M;\ -\infty<z<\infty) \tag{30}$$

where ε_{ji}^d is obtained from (7-14) by replacing ε_{zz}^d, a_n, b_n, N, r, θ in (7-9) by ε_{ji}^d, a_{jn}, b_{jn}, N_j, b_j, θ_j; b_o, p, b_n, N, r_o, Z in (11-13) by b_{jo}, p_j, b_{jn}, N_j, r_j, Z_j; b, θ, N in (14) by b_j, $\theta-\theta_j$, N_j, and $\cos(nN\theta)$ in (12) by $\cos[nN_j(\theta-\theta_j)]$. Note that ε_{ji}^c and ε_{ji}^d are dependent on $Z_i(z)$ only.

To evaluate ε_j^c the interaction of two different fibers at two arbitrary locations has to be established. We first

observe that ε^c_{jj} which appears in (29) is given by (5). For this all one needs to do is to replace $\varepsilon_z{}^c$, b, Z, N, ρ_o, and r_o in (5) by ε^c_{jj}, b_j, Z_j, N_j, ρ_j and r_j, respectively. Referring now to Figures 3 and 2c and the basic concentrated load solution [1,4], the axial strain at the point $r = b_j$, $\theta = \theta_j$, z due to N_i line loads $2\pi r_i Z_i(t)$, acting along $r = b_i$, $\theta = \theta_{im} = \theta_i + \frac{2\pi m}{N_i}$, $z = t$, $(m = 1,..,N_i, -\infty<t<\infty)$ may be expressed as

$$\varepsilon^c_{ji}(b_j,\theta_j,z) = \frac{\pi r_i}{EC_1} \int_{-\infty}^{\infty} Z_i(t)(t-z) \sum_{m=1}^{N_i} \left\{ \frac{1-2\gamma}{[d_{im}^2 + (t-z)^2]^{3/2}} + \frac{3\gamma(t-z)^2}{[d_{im}^2 + (t-z)^2]^{5/2}} \right\} dt, \quad (i\neq j, -\infty<z<\infty) \qquad (31)$$

where

$$\gamma = 1/(3-4\nu), \quad C_1 = 4\pi(1-\nu)/[(1+\nu)(3-4\nu)],$$

$$d_{im}^2 = b_j^2 + b_i^2 - 2b_j b_i \cos\left(\theta_i + \frac{2\pi m}{N_i} - \theta_j\right), \quad (m = 1,..,N_i)$$

If we now substitute (with the necessary change in notation) from(2, 4, 6, 29-31) into (28) we obtain a system of singular integral equations of the following form for unknown functions $Z_1,..,Z_M$:

$$\frac{1}{EC_1} \int_{-\infty}^{\infty} \frac{Z_j(t)}{t-z}\, dt + \int_{-\infty}^{\infty} \sum_{i=1}^{M} k_{ji}(z,t)Z_i(t)dt = f_j(z),$$

$$(j = 1,..,M; \ -\infty<z<\infty). \qquad (32)$$

where f_j and k_{ji}, $(i,j = 1,..,M)$ are known functions. After solving (32) the interface shear stresses, the fiber stresses, the crack surface displacement, and the stress intensity factor may be obtained from expressions similar to (16), (17), (with 18-21), (25) and (27). For example, the stress intensity

factor may be expressed as

$$k_1(\theta) = (2/\pi)\{\sigma_o + \sum_{j=1}^{M} \sum_{n=0}^{\infty} a_{jn}\, b_{jn} \cos[nN_j(\theta-\theta_j)]\}, (0 \leq \theta < 2\pi) \quad (33)$$

where a_{jn} and b_{jn} are obtained from (10-13) by replacing a_n, b_n, N, p, b, θ, Z, r_o by a_{jn}, b_{jn}, N_j, p_j, b_j, $\theta-\theta_j$, Z_j, r_j, respectively.

4. ON THE SOLUTION OF INTEGRAL EQUATIONS

The integral equations (15) and (32) represent special cases of the following more general system:

$$Ag(x) + \frac{B}{\pi i} \int_{-\infty}^{\infty} \frac{g(t)}{t-x}\, dt + \int_{-\infty}^{\infty} K(x,t)g(t)dt = f(x), \quad (-\infty<x<\infty), \quad (34)$$

$$A = (a_{ij}),\ B = (b_{ij}),\ g(x) = (g_i(x)),$$

$$K(x,t) = (k_{ij}(x,t)),\ f(x) = (f_i(x)),\ (i,j = 1,..,n),$$

where the matrices A and B are constant and are such that A+B and A-B are nonsingular, the known functions f_i and k_{ij} and the unknown functions g_i may be complex, and the kernels k_{ij} satisfy the necessary regularity conditions at infinity. The system of singular integral equations (34) may formally be regularized as follows: Define the following holomorphic functions:

$$G(z) = \frac{1}{2\pi i} \int_{-\infty}^{\infty} \frac{g(t)}{t-z}\, dt, \qquad z = x + iy, \quad (35)$$

$$H(z) = \begin{cases} G(z), & z \in S^+ \\ (A+B)^{-1}(A-B)G(z), & z \in S^-, \end{cases} \quad (36)$$

$$G(z) = (G_j(z)),\ H(z) = (H_j(z)),\ (j = 1,..,n),$$

$$(A-B)^{-1} = C = (c_{ij}),\ (A+1)^{-1} = D = (d_{ij})$$

In terms of the sectionally holomorphic functions $H_j(z)$ (34) may be expressed as

$$H^+(x) - H^-(x) = D[f(x) - \int_{-\infty}^{\infty} K(x,t)g(t)dt]. \qquad (37)$$

The solution of (37) is [5]

$$H(z) = \frac{D}{2\pi i} \int_{-\infty}^{\infty} [f(s) - \int_{-\infty}^{\infty} K(s,t)g(t)dt] \frac{ds}{s-z} + P(z), \qquad (38)$$

where $P(z) = (P_j(z))$, $(j=1,..,n)$ is an arbitrary (matrix) polynomial which must be identically zero because of the condition that $F(z)\to 0$ for $|z|\to\infty$. The solution of (34) may then be expressed as

$$g(x) = G^+(x) - G^-(x) = H^+(x) - C(A+B)H^-(x), \qquad (39)$$

giving

$$g(x) + \int_{-\infty}^{\infty} M(x,t)g(t)dt = p(x), \quad (-\infty<x<\infty) \qquad (40)$$

where

$$M(x,t) = (m_{jk}(x,t)) = (D+C)K(x,t) + \frac{D-C}{2\pi i} \int_{-\infty}^{\infty} \frac{K(s,t)}{s-x} ds,$$

$$p(x) = (p_j(x)) = \frac{D+C}{2} f(x) + \frac{D-C}{2\pi i} \int_{-\infty}^{\infty} \frac{f(s)}{s-x} ds,$$

$$(j,k = 1,..,n). \qquad (41.a,b)$$

It should be emphasized that the objective of the regularization process is "smoothing" the kernels. Thus the system of singular integral equations (34) is reduced to that of Fredholm integral equations given by (40). It is seen that if (34) consists of its dominant part only, i.e., if $K(x,t) = 0$, then (40) and (41.b) give the solution in closed form. If K is not zero and the integral in (40) is one of the standard convolution

types (see, for example, [6]) the solution of (40) may again be obtained in closed form. Otherwise (40) may have to be solved numerically.

From the view point of numerical analysis the procedure outlined here which leads to (40) would be very appropriate and convenient provided the kernels m_{ij} can be evaluated in closed form. If these kernels too have to be evaluated numerically from the singular integrals given by (41.a), the technique could be quite laborious. In this case the following simpler and more direct approach may be preferable: Noting that

$$\int_{-\infty}^{\infty} \frac{dt}{t-x} = 0, \quad (-\infty<x<\infty) \tag{42}$$

equation (34) may be expressed as

$$Ag(x) + \frac{B}{\pi i} \int_{-\infty}^{\infty} \frac{g(t)-g(x)}{t-x}\, dt + \int_{-\infty}^{\infty} K(x,t)g(t)dt = f(x), \quad (-\infty<x<\infty) \tag{43}$$

It should be pointed out that because of the nature of the related physical problems, unlike the solution of the singular integral equations defined on non-intersecting smooth arcs, the solution of singular integral equations defined on infinite lines and smooth closed contours are usually bounded and continuous functions. Hence, for the purpose of numerical analysis, in the latter type equations the singularity of the kernel can always be removed as in (43) and the resulting system can be treated as ordinary Fredholm integral equations. Note that in (43) for t=x the integrand in the second term becomes the derivative of g(t) at x which is assumed to be bounded.

In solving (43) one may still encounter numerical difficulties because of the fact that the support of the integral equations is infinite. To overcome this usually a simple change in variables such as the following would be sufficient:

$$t = \tan\frac{\pi r}{2},\ x = \tan\frac{\pi s}{2},\ (-\infty<(t,x)<\infty,\ -1<(r,s)<1) \tag{44}$$

Also, to improve the effectiveness of the numerical solution, it is preferable to use a Gaussian-type integration formula rather than one based on dividing the domain into equal subintervals. In the type of problems under consideration an appropriate integration formula would be the following Gauss-Legendre formula:

$$\int_{-1}^{1} F(r)dr = \sum_{j=1}^{n} w_j F(r_j), \tag{45}$$

where

$$P_n(r_j) = 0,\ w_j = \frac{2}{(1-r_j)^2[P_n'(r_j)]^2},\ (j = 1,..,n).$$

After making the transformation (44), (43) becomes

$$Ag_1(s) + \frac{B}{\pi i}\int_{-1}^{1} \frac{g_1(r) - g_1(s)}{\tan\frac{\pi r}{2} - \tan\frac{\pi s}{2}} \frac{dr}{\cos^2\frac{\pi r}{2}} + \int_{-1}^{1} K_1(s,r)g_1(r)\frac{dr}{\cos^2\frac{\pi r}{2}} = f_1(s),\ (-1<x<1) \tag{46}$$

where $g_1(s) = g(\tan\pi s/2)$, etc. First it may be noted that the regularity condition of the problem requires $K(x,t)$ to decay sufficiently fast so that the second integral in (46) is convergent. Hence, the application of (45) to this integral will

be straightforward. Unlike the Gauss-Chebyshev integration formulas, in the application of Gauss-Legendre formula to the solution of integral equations both variables s_i and r_j are taken to be the roots of the same polynominal, i.e.,

$$P_n(s_i) = 0,\ P_n(r_j) = 0,\ (i,j = 1,..,n). \tag{47}$$

this means that at i=j the second integral in (46) may need some care. Observing that

$$\lim_{s\to r} \frac{g_1(r) - g_1(s)}{(\tan\frac{\pi r}{2} - \tan\frac{\pi s}{2})\cos^2\frac{\pi r}{2}} = \frac{2}{\pi}\frac{dg_1(r)}{dr},$$

this difficulty may easily be circumvented by replacing the integrand in the second term for i=j by

$$\frac{2}{\pi}\frac{g_1(r_{i+1}) - (g_1(r_{i-1})}{r_{i+1} - r_{i-1}}\ .$$

Thus, writing (46) at n locations s_i one obtains a system of n (matrix) equations for the unknowns $g_1(s_i)$, (i=1,..,n).

5. NUMERICAL RESULTS

Figures 4-13 show some of calculated results(*). Figure 4 shows a typical result giving the body force distribution Z(z) for a single fiber,(i.e,N=1) obtained from (15). Note that because of symmetry with respect to z=0 plane Z is an odd and the fiber stress σ_f is an even function of z. A sample result giving the distribution of the stress intensity factor along the crack border for various values of N, the number of fibers in a single set is shown in Figure 5. As in the

---

* Further results and the details of the analysis may be found in [7].

case of filament reinforcements, as N increases the θ-dependence of the stress intensity factor decreases. Hence, for large values of N, for the purpose of analyzing the effect of the fiber reinforcement on the stress intensity factor, one may treat the problem as being axisymmetric. This may be done by assuming that the matrix is reinforced by a cylindrical membrane having the same modules E_f as the fibers and an equivalent cross-sectional area (i.e., $N\pi r_o^2$). Figure 6 shows the result of such an axisymmetric analysis where it is assumed that N=16. It is seen that as the (fiber) distance b increases, the effect of the reinforcement rapidly decreases, the stress intensity factor ratio $k_1/(2\sigma_o\sqrt{a}/\pi)$ approaching the value for the penny-shaped crack without reinforcement. For smaller values of b as the crack border approaches the fibers the problem cannot be treated as axisymmetric regardless of the number N. However, the membrane reinforcement has a physical meaning. In this case when the crack touches the reinforcement the power of stress singularity (see equation (26)) becomes less than $-\frac{1}{2}$, and therefore the stress intensity factor as defined by (26) would be expected to go to zero. This trend is clearly seen in Figure 6.

Figure 7 gives some idea about the reinforcement effect of two fibers placed in different locations ($b_1=1.4a$, $b_2=1.5a$, $\theta_1=0$, $\theta_2=0.4\pi$). In this and in the subsequent examples the two sets of fibers are assumed to have equal radii ($r_1=r_2=r_o$) and stiffnesses ($E_1=E_2=E_f$). The effect of the number of fibers in

each set is shown in Figure 8 where it is assumed that $b_1=1.4a$, $b_2=1.5a$, $N_1=N_2=N$, $r_1=r_2=0.2a$, $E_f=130E$, and $\theta_1=0$, $\theta_2=\pi/4$. It is seen that as N increases the θ-dependence as well as the magnitude of the stress intensity factor again decreases. Typical results giving the distribution of the body forces Z_1, Z_2 and fiber stresses σ_{1f} and σ_{2f} for the two fibers are shown in Figures 9 and 10. $E_f=15E$ used in these figures approximately correspond to steel-concrete combination. Note that at distances beyond a few crack radii Z_1 and Z_2 die out quite rapidly and σ_{1f} and σ_{2f} approach the value of $\sigma_o E_f/E$ corresponding to the fiber stress in uncracked reinforced matrix.

In the case of multiple set of fibers too for large values of N_i the problem may be treated as axisymmetric by replacing the individual sets of fibers by equivalent elastic cylindrical membranes. Figures 11-13 show some of the results obtained under this assumption for two sets of fibers. In these examples the membranes are assumed to be equivalent to 8 fibers in each set. Figure 11 shows the effect of the fiber radius $r_1=r_2=r_o$ and Figure 12 shows the effect of the modulus ratio E_f/E on the stress intensity factor which is seen to decrease with both increasing r_o and increasing E_f/E. Figure 13 shows the effect of the fiber distance b_2 for a fixed b_1 on the stress intensity factor k_1. The asymptote shown by the dashed line is the stress intensity factor corresponding to a single set of fibers at b_1. It is seen that

k_1 rapidly approaches this asymptotic value as b_2 increases. This implies that the sets of fibers which may exist in the composite beyond a certain distance from the crack would have only a negligible effect on the stress intensity factor. The figure also shows that as b_2 decreases the reduction in the stress intensity factor, k_1 becomes more significant and again k_1 would approach zero as the distance from the crack front to the reinforcing membrane goes to zero.

Comparing the results obtained in this paper for the reinforcing fibers with that found in [2] for finite filaments it may be remarked that there is considerable qualitative similarity regarding the distribution of the stress intensity factor. However, in the filament case the interface shear (or the body force Z) is concentrated around the filament ends and generally gives rise to filament stresses which are higher than the stresses found in the fibers. As a result the reinforcement effect (measured by the reduction in the stress intensity factor) of the filaments is relatively higher than that of the comparably distributed fibers.

REFERENCES

1. Erdogan, F. and Pacella, A.H., "A penny-shaped crack in a filament-reinforced matrix--I. The filament model", Int. J. Solids Structures, Vol. 10, p. 785 (1974).

2. Pacella, A.H. and Erdogan, F., "A penny-shaped crack in a filament-reinforced matrix--II. The crack problem", Int. J. Solids Structures, Vol. 10, p. 807 (1974).

3. Watson, G.N., A Treatise on the Theory of Bessel Functions, Cambridge University Press, (1944).

4. Love, A.E.H., A Treatise on the Mathematical Theory of Elasticity, Dover Publ. New York (1944).

5. Muskhelishvili, N.I. Singular Integral Equations, Noordhoff N.V. Groningen, Holland (1953).

6. Titchmarsh, E.C., Introduction to the Theory of Fourier Integrals, Oxford Univ. Press (1937).

7. Narayanan, T.V., "A penny-shaped crack in an infinite matrix reinforced by infinite fibers", Ph.D. Dissertation, Lehigh University, (1973).

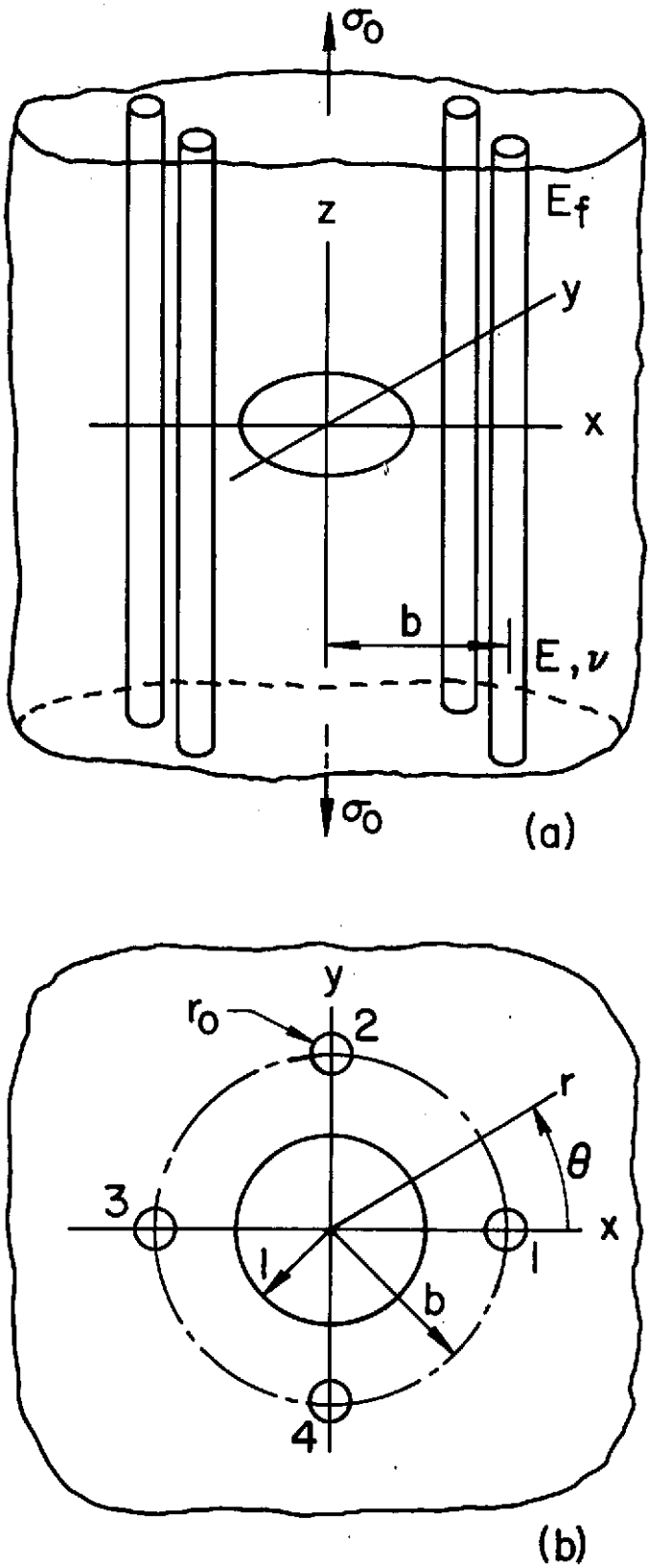

Figure 1. Geometry for the penny-shaped crack in an elastic matrix reinforced by symmetrically located elastic fibers.

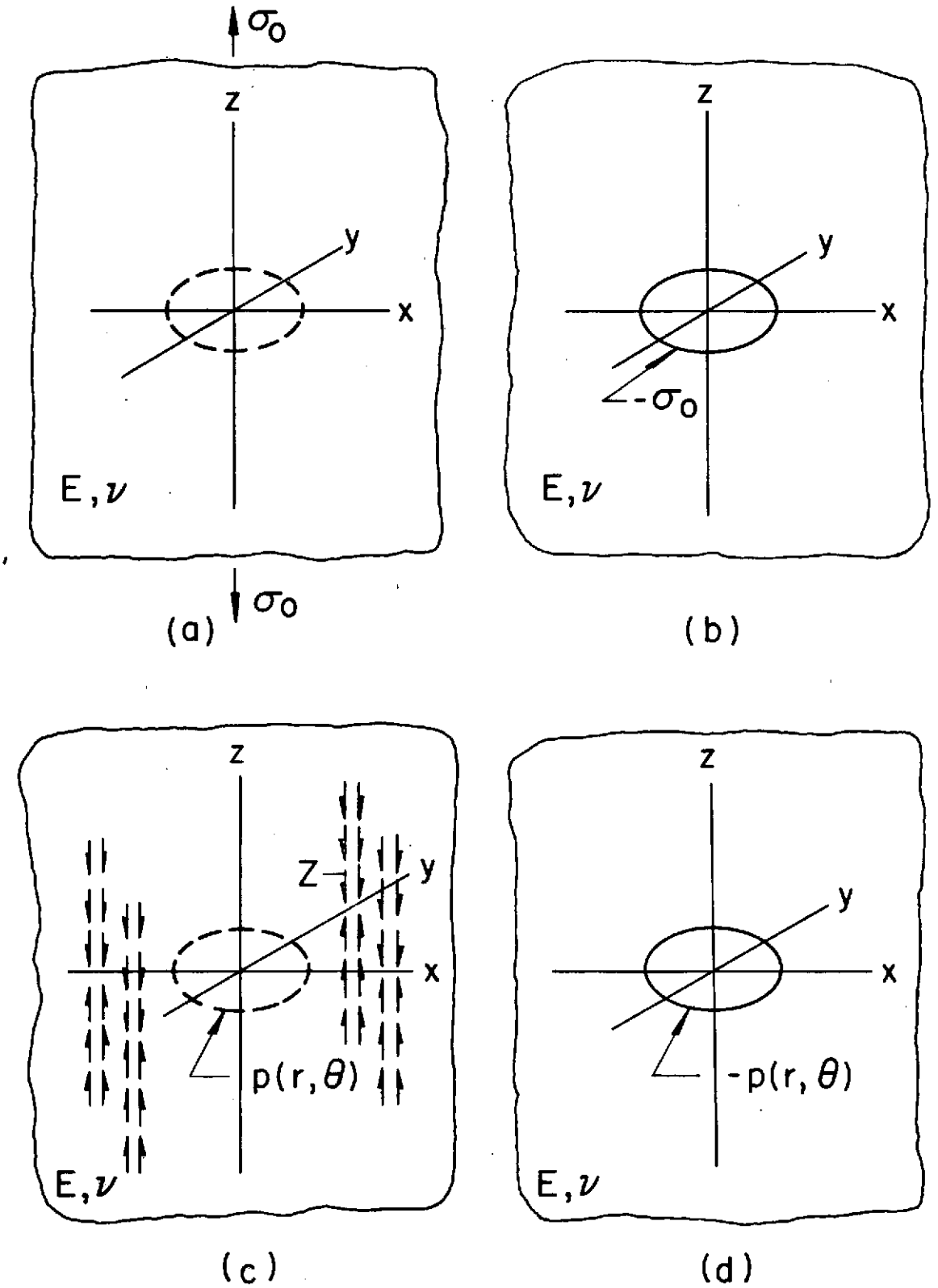

Figure 2. Superposition for the stresses and displacements in the matrix.

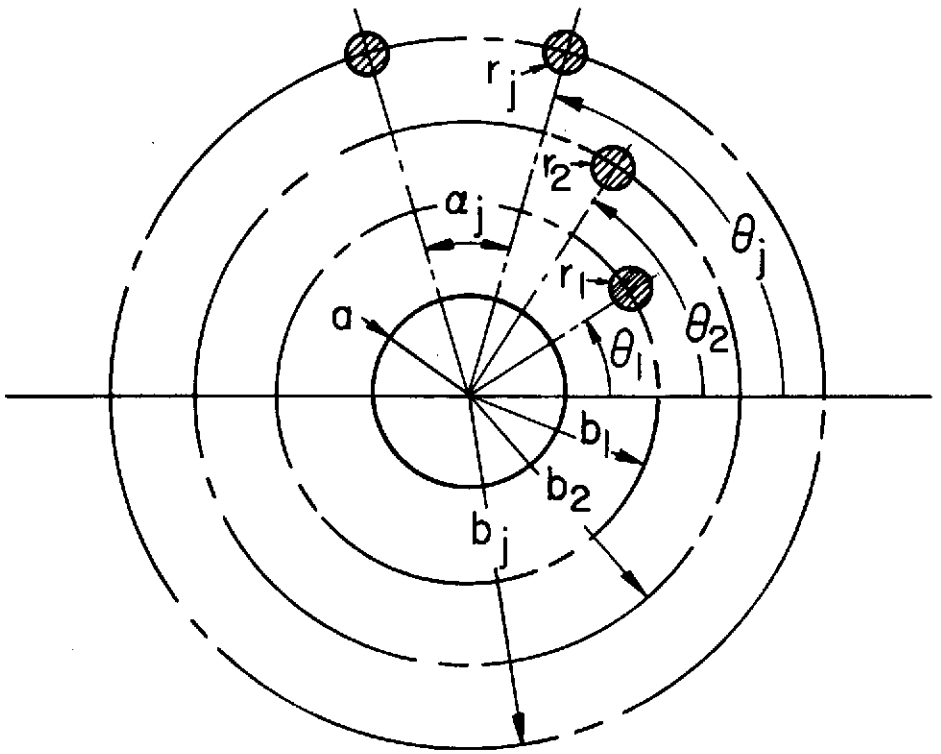

Figure 3. Geometry of the multiple set of fibers; M is the number of concentric rings containing the fibers; in each ring the fibers are equally spaced with $\alpha_j = 2\pi/N_j$, N_j being the number of fibers in the jth ring.

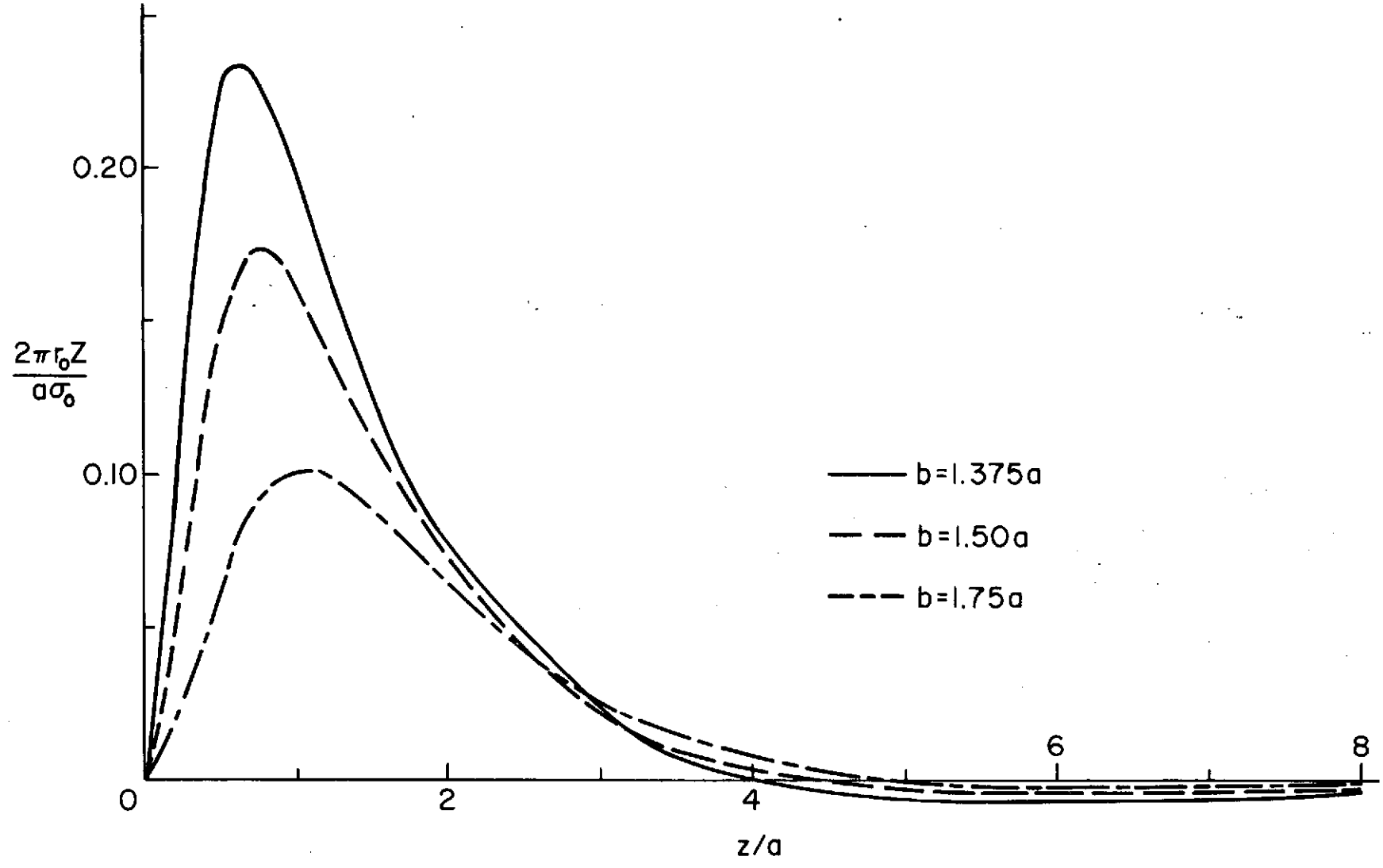

Figure 4. Distribution of body force Z(z) for E_f=130E, ν=0.35, r_0=0.15a, and (_____): b=1.375a, (------): b=1.50a, (___ . ___ . ___): b=1.75a.

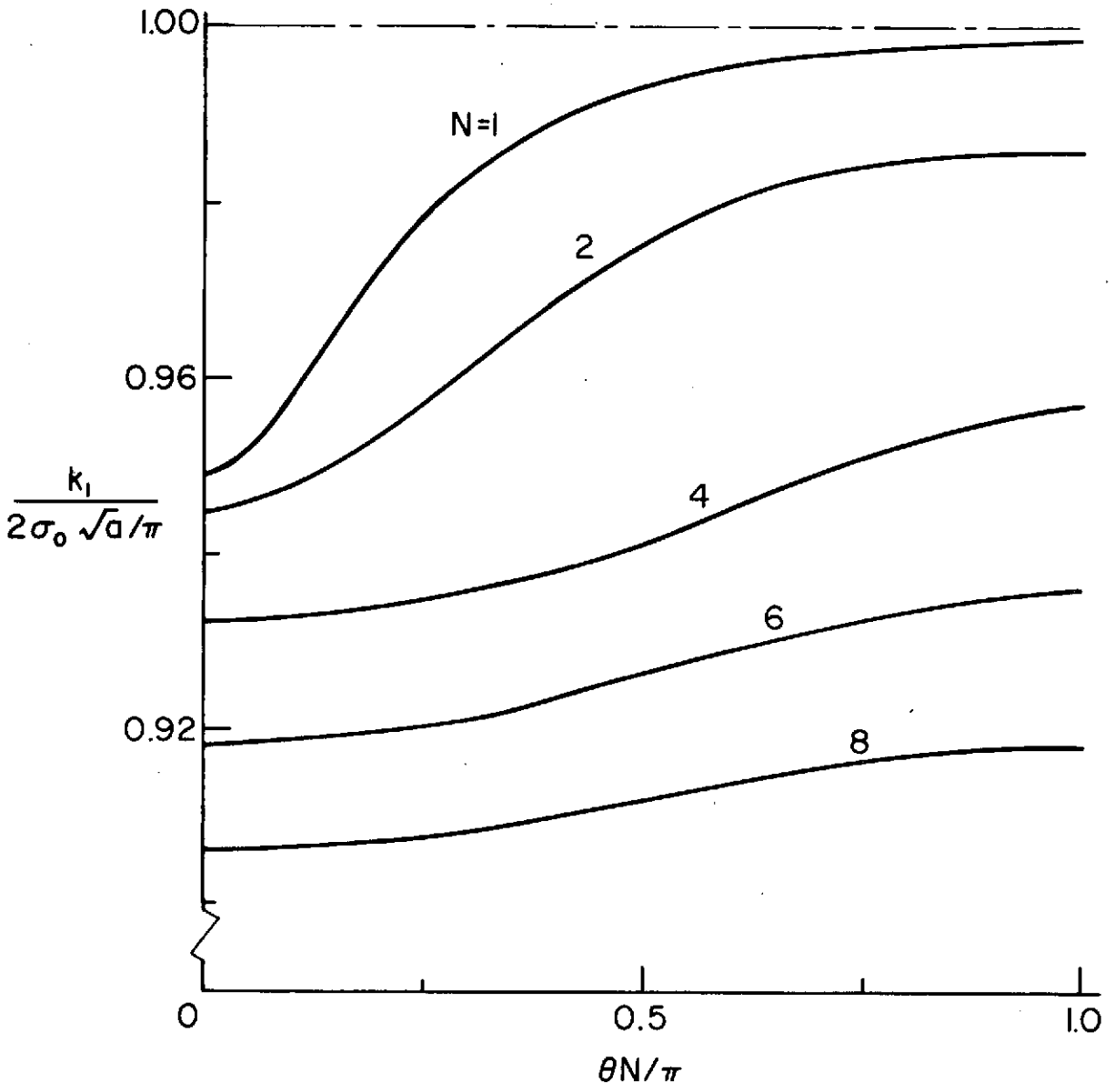

Figure 5. Effect of the number of fibers N on the stress intensity factor distribution along the crack border; b=1.375a, r_o=0.15a, ν=0.35, E_f=130E.

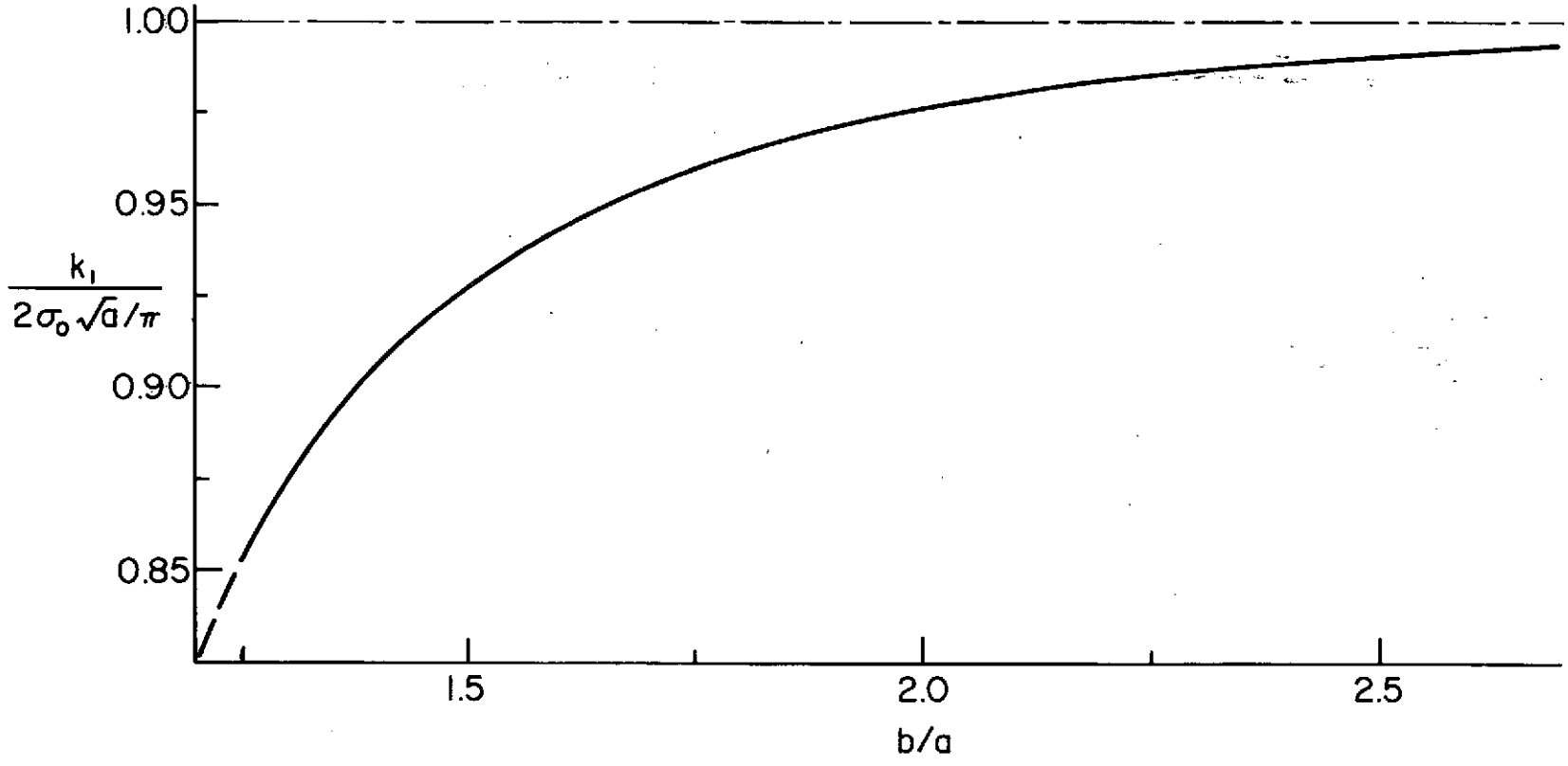

Figure 6. Effect of the fiber distance b on the stress intensity factor for the axisymmetric case; N=16, r_o=0.1a, E_f=130E, ν=0.35.

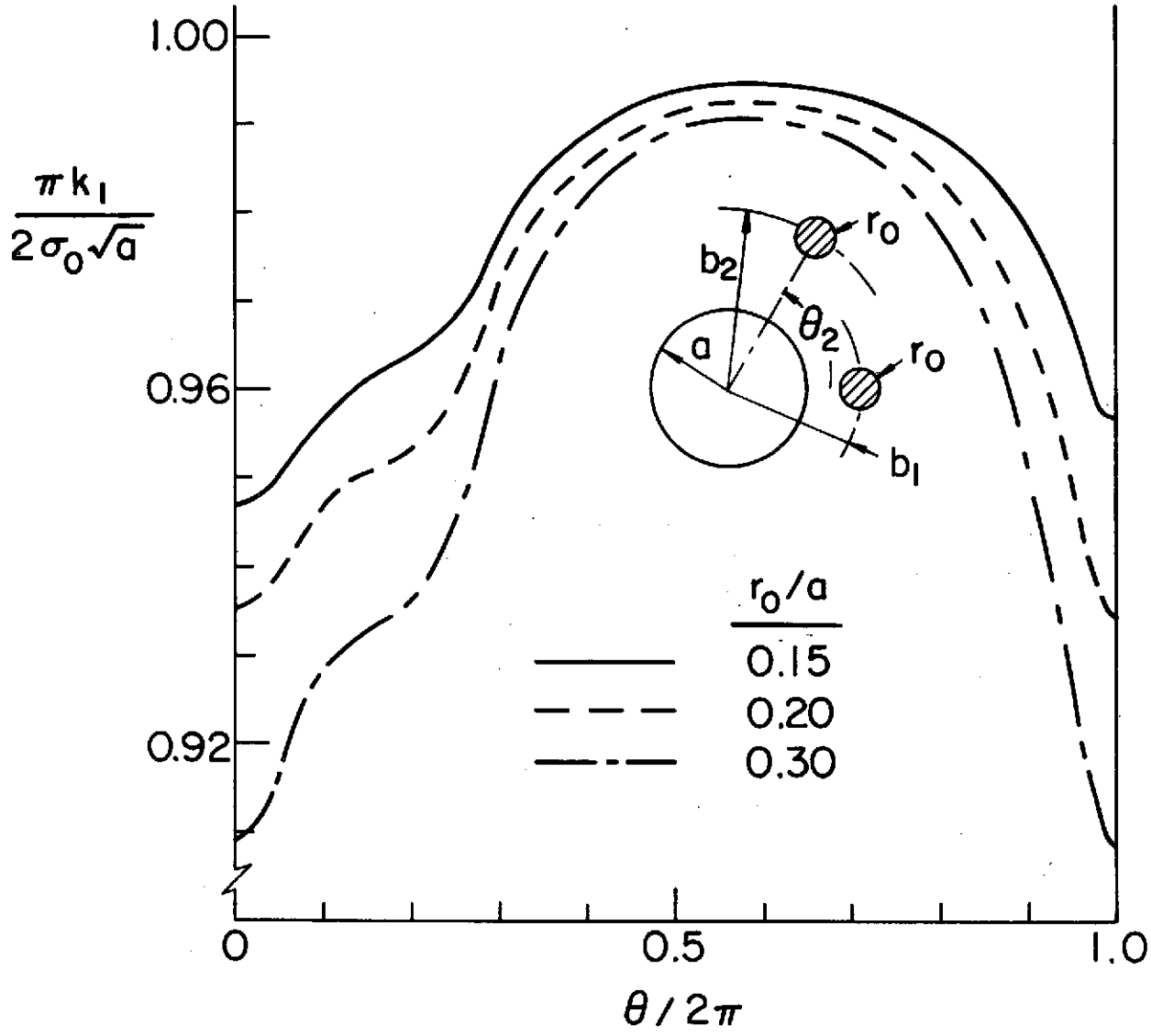

Figure 7. Angular variation of the stress intensity factor for reinforcement by two fibers; $b_1=1.4a$, $b_2=1.5a$, $\theta_1=0$, $\theta_2=0.4\pi$, $E_1=E_2=130E$, $\nu=0.35$, $r_1=r_2=r_o$, and (_____): $r_o=0.15a$, (_ _ _ _): $r_o=0.20a$, (_._._): $r_o=0.30a$.

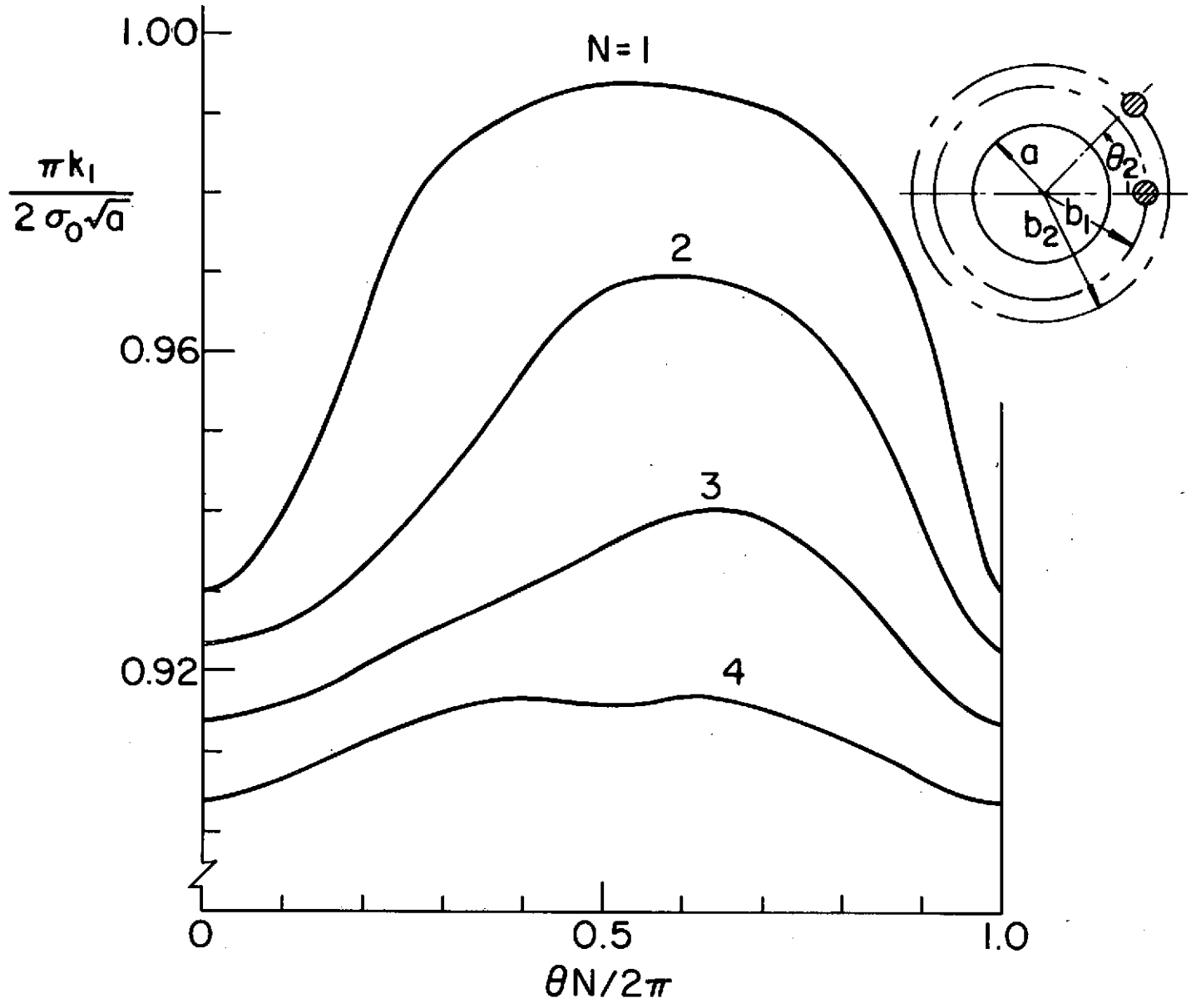

Figure 8. Angular variation of the stress intensity factor for two sets of reinforcing fibers; $b_1=1.4a$, $b_2=1.5a$, $\theta_1=0$, $\theta_2=\pi/4$, $E_1=E_2=130E$, $\nu=0.35$, $r_1=r_2=0.2a$, $N_1=N_2=N=8$.

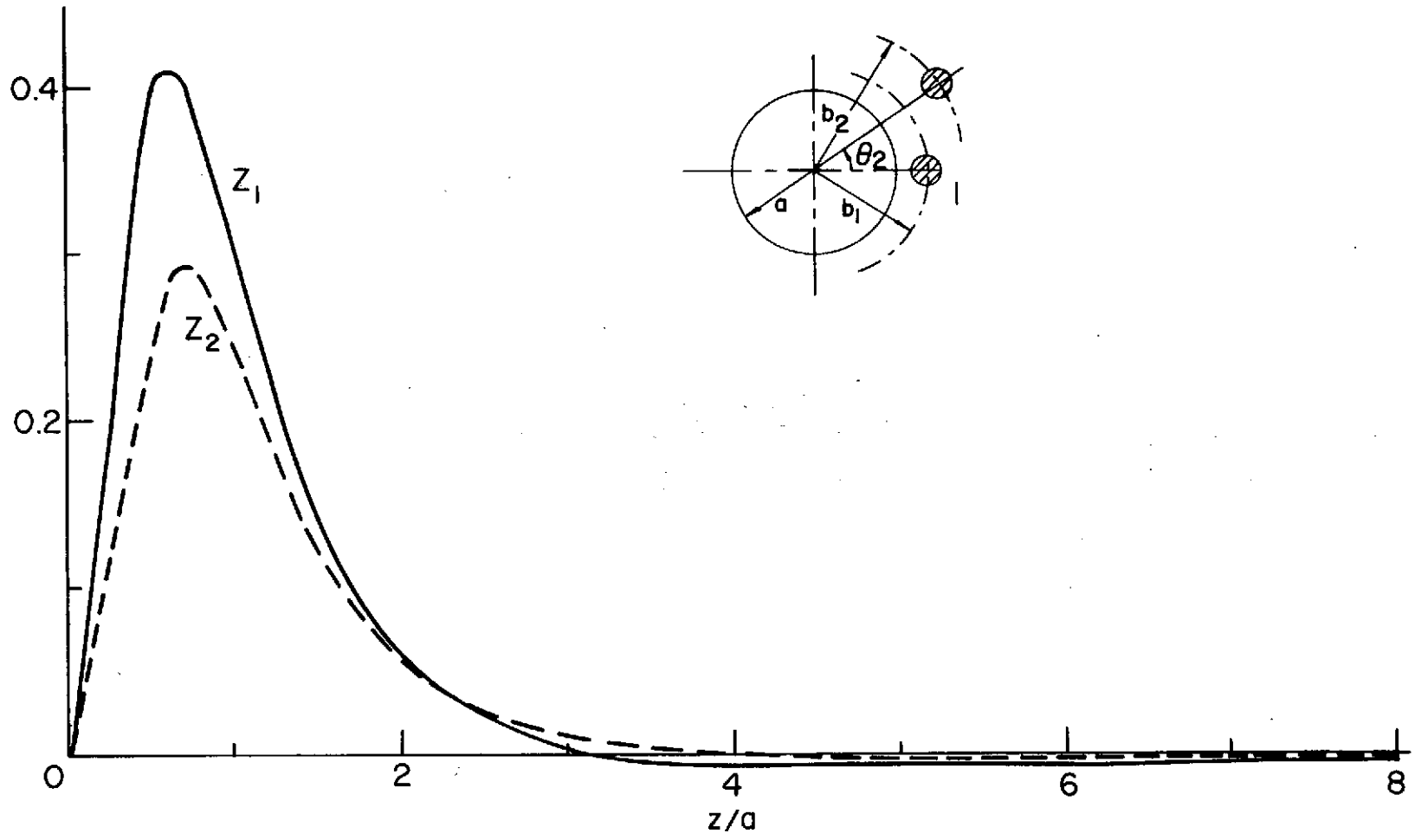

Figure 9. Distribution of body forces for reinforcement by two fibers; $b_1=1.5a$, $b_2=1.6a$, $r_1=r_2=0.4a$, $\theta_1=0$, $\theta_2=0.2\pi$ $E_1=E_2=15E$.

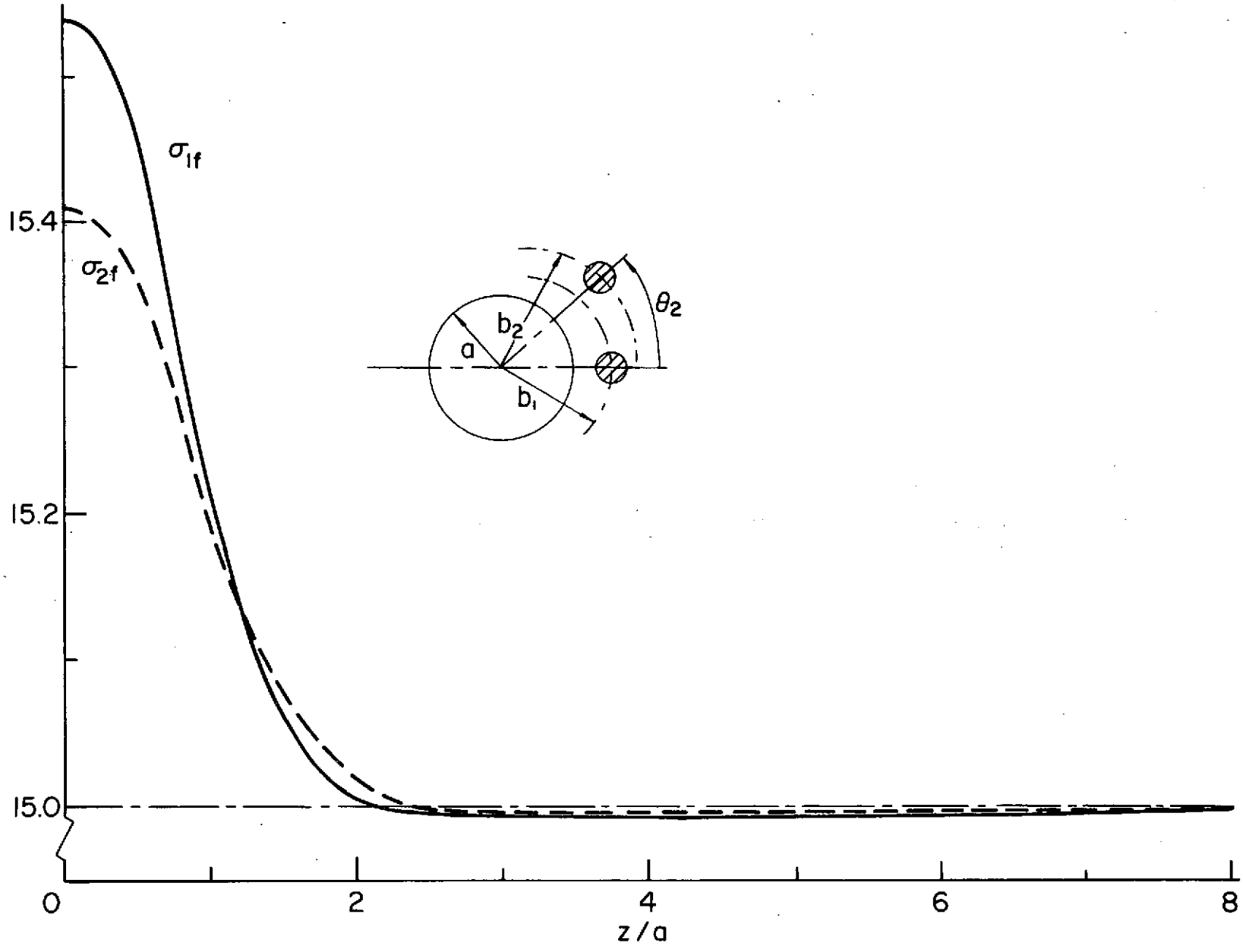

Figure 10. Distribution of fiber stress σ_f for reinforcement by two fibers; $b_1=1.5a$, $b_2=1.6a$, $r_1=r_2=0.4a$, $\theta_1=0$, $\theta_2=0.2\pi$, $E_1=E_2=15E$.

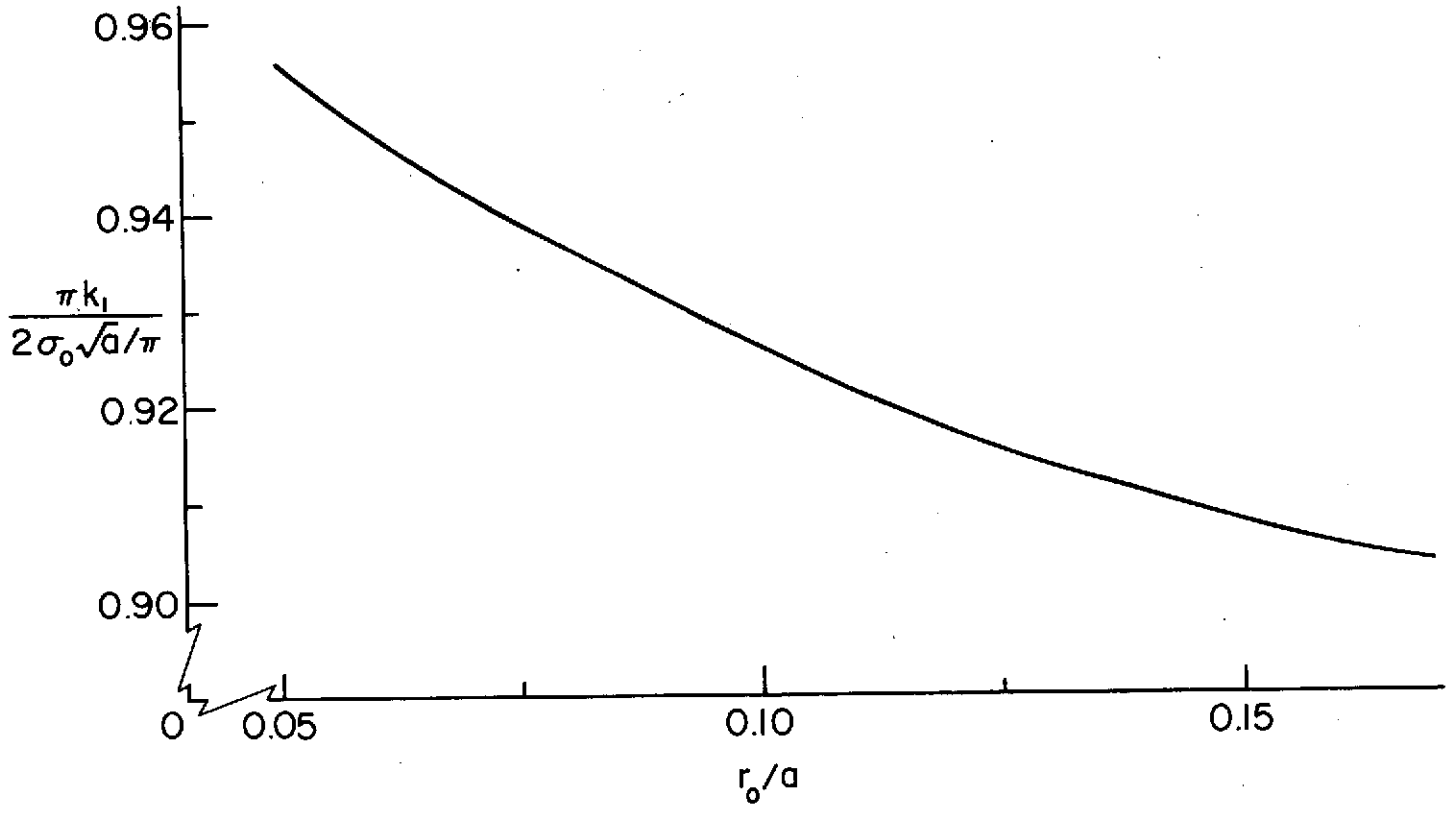

Figure 11. Effect of fiber radius $r_0=r_1=r_2$ on the stress intensity factor for reinforcement by two sets of fibers obtained from the axisymmetric solution, $N_1=N_2=8$, $b_1=1.4a$, $b_2=1.6a$, $E_1=E_2=130E$, $\nu=0.35$.

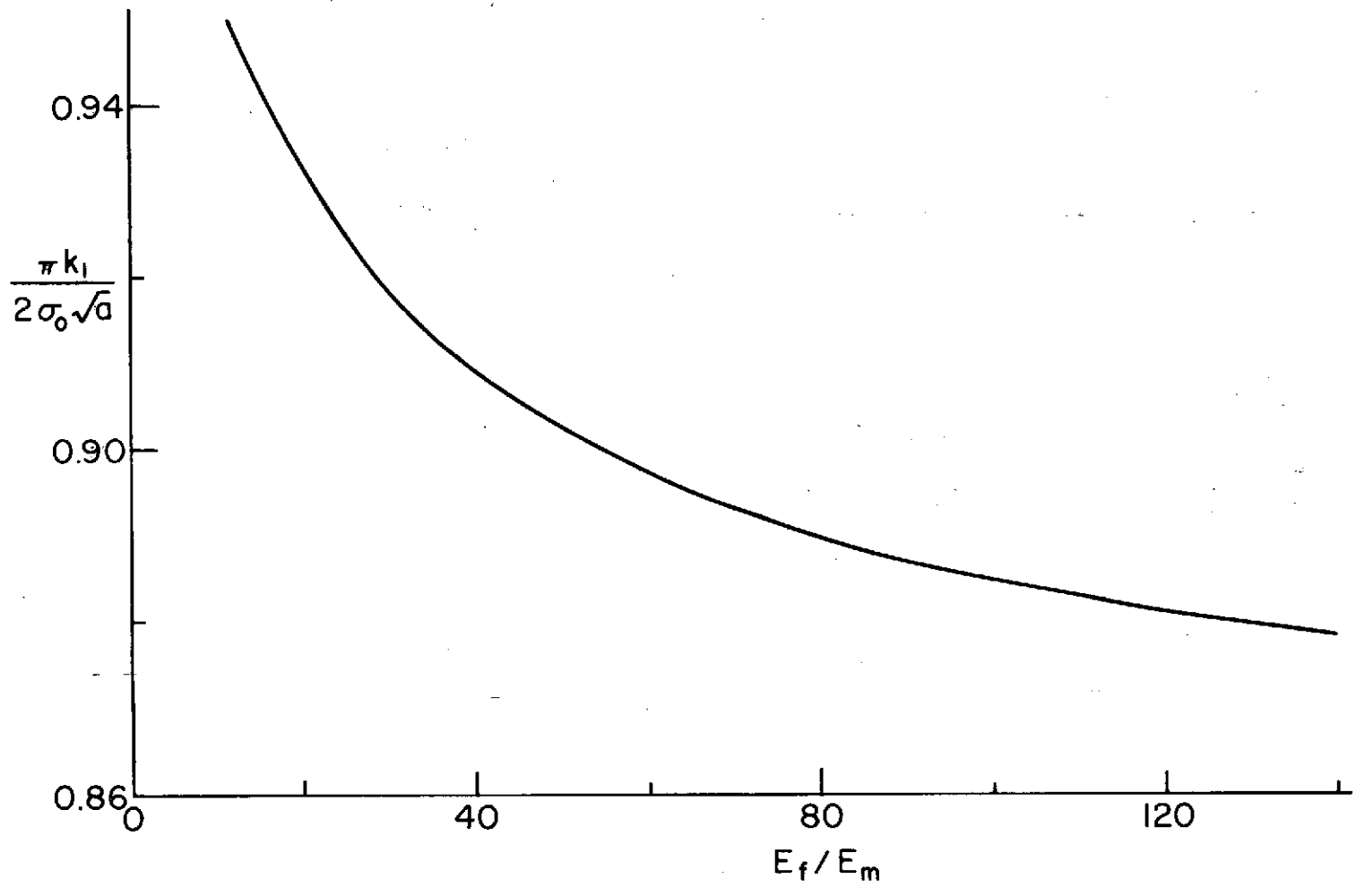

Figure 12. Effect of modulus ratio E_f/E on the stress intensity factor for reinforcement by two sets of fibers obtained from the axisymmetric solution; $E_1=E_2=E_f$, $\nu=0.35$, $N_1=N_2=8$, $b_1=1.25a$, $b_2=1.5a$, $r_1=r_2=0.1a$.

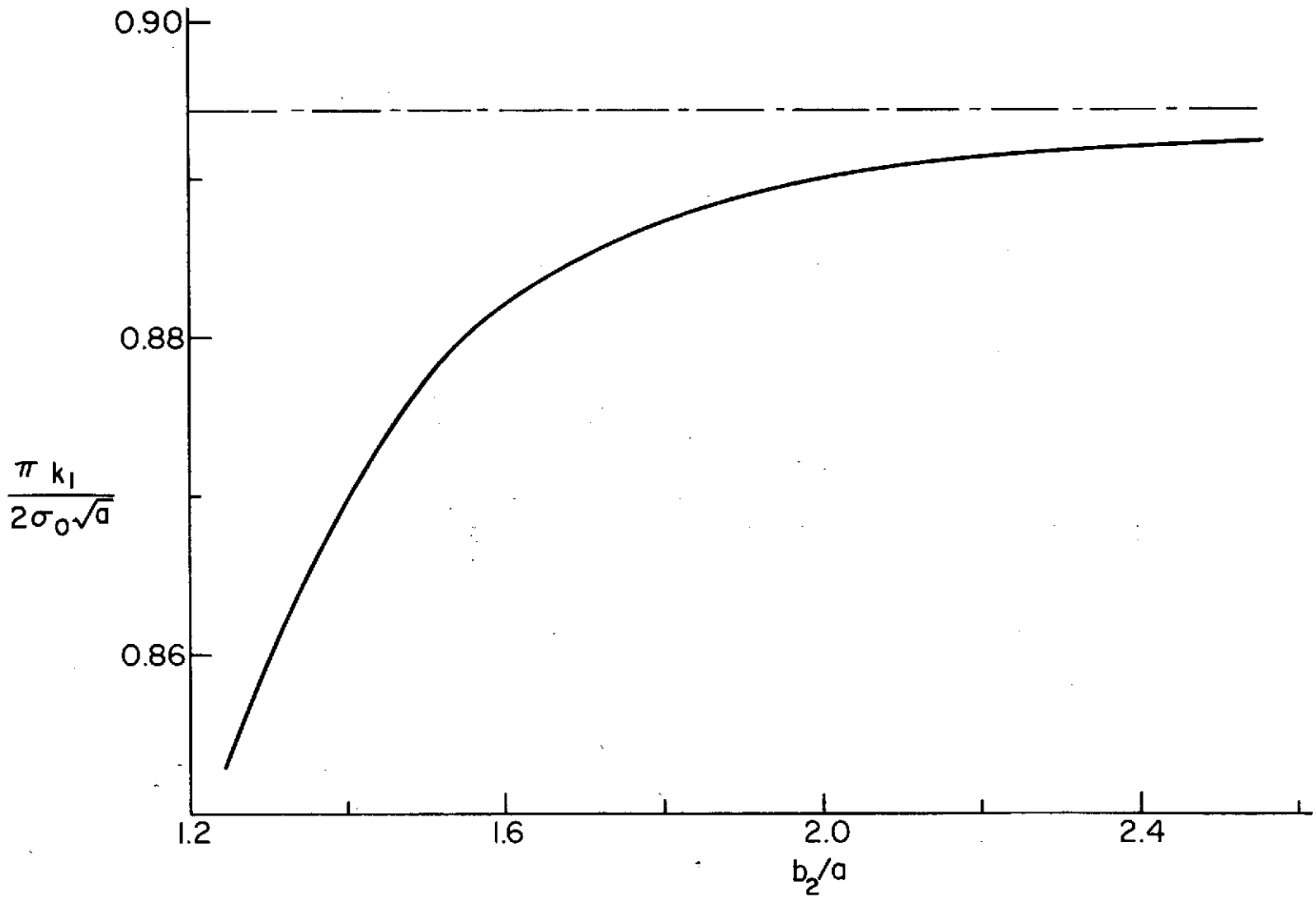

Figure 13. Effect of fiber distance b_2 on the stress intensity factor for reinforcement by two sets of fibers obtained from the axisymmetric solution; $N_1=N_2=8$, $E_1=E_2=130E$, $\nu=0.35$, $b_1=1.25a$, $r_1=r_2=0.1a$.